- We report a novel protective action of estrogen on the BBB.
- Estrogen enhances inter-endothelial cell tight junction function.
- Estrogen's actions are mediated by GPR30 signalling and phosphorylation of annexin A1.
- Estrogen limits lymphocyte extravasation after challenge with inflammatory cytokines.
- Estrogen limits inflammation-induced immune cell trafficking through ERβ/annexin A1 pathways

Estrogen protects the blood-brain barrier from inflammation-induced disruption and increased lymphocyte trafficking

Maggioli, E.[a/1], McArthur, S.[a/b/1], Mauro, C.[a], Kieswich, J.[a], Kusters, DHM.[c/d], Reutelingsperger, CPM.[c], Yaqoob, M.[a] & Solito, E.[a/2]

[a]William Harvey Research Institute, Barts and the London School of Medicine and Dentistry, Queen Mary University of London, Charterhouse Square, London EC1M 6BQ, UK. [b]Department of Biomedical Sciences, Faculty of Science & Technology, University of Westminster, New Cavendish Street, London, W1W 6UW, UK. [c]Cardiovascular Research Institute, and Department of Biochemistry, Maastricht University, 6200 Maastricht, the Netherlands. [d]Department of Pathology, University of Michigan Health System, 109 Zina Pitcher Place, 4062 BSRB, Ann Arbor, MI 48109-2200.

[1]EM and SMcA contributed equally to this work.

[2]*Correspondence* to Egle Solito, Centre for Translational Medicine and Therapeutics, William Harvey Research Institute, Barts and the London School of Medicine and Dentistry, Queen Mary University of London, Charterhouse Square, London EC1M 6BQ, UK. (e.solito@qmul.ac.uk)

Keywords - Blood-brain barrier, estrogen, tight junction, Annexin A1, lymphocytes.

ABSTRACT

Sex differences have been widely reported in neuroinflammatory disorders, focusing on the contributory role of estrogen. The microvascular endothelium of the brain is a critical component of the blood-brain barrier (BBB) and it is recognised as a major interface for communication between the periphery and the brain. As such, the cerebral capillary endothelium represents an important target for the peripheral estrogen neuroprotective functions, leading us to hypothesise that estrogen can limit BBB breakdown following the onset of peripheral inflammation.

Comparison of male and female murine responses to peripheral LPS challenge revealed a short-term inflammation-induced deficit in BBB integrity in males that was not apparent in young females, but was notable in older, reproductively senescent females. Importantly, ovariectomy and hence estrogen loss recapitulated an aged phenotype in young females, which was reversible upon estradiol replacement. Using a well-established model of human cerebrovascular endothelial cells we investigated the effects of estradiol upon key barrier features, namely paracellular permeability, transendothelial electrical resistance, tight junction integrity and lymphocyte transmigration under basal and inflammatory conditions, modelled by treatment with TNFα and IFNγ. In all cases estradiol prevented inflammation-induced defects in barrier function, action mediated in large part through up-regulation of the central coordinator of tight junction integrity, annexin A1. The key role of this protein was then further confirmed in studies of human or murine annexin A1 genetic ablation models.

Together, our data provide novel mechanisms for the protective effects of estrogen, and enhance our understanding of the beneficial role it plays in neurovascular/neuroimmune disease.

1. Introduction

Several lines of evidence suggest that the sex differences seen in vascular and neural diseases may be at least partly linked to differing sex hormone complements. In particular, a number of beneficial effects have been attributed to the principal female hormone estrogen, including in conditions as diverse as Parkinson's disease, Alzheimer's disease, head injury and multiple sclerosis (1). One important working hypothesis is that the neuroprotective effects of estrogen may be related to its known anti-inflammatory and immunomodulatory actions (2, 3).

The endothelium of the blood-brain barrier (BBB) is at the forefront of the defensive features of the central nervous system, regulating its interactions with the immune system. In particular, there is accumulating evidence that BBB function is compromised during peripheral inflammation, leading to inappropriate passage of cells and molecules into the brain parenchyma (4). Estrogen has been shown to exert a variety of anti-inflammatory effects, including reducing iNOS activity (5), directly regulating the cytokine milieu (6) and altering expression of vascular and leukocyte adhesion molecules (7). Whilst initial studies have identified estrogen as being able to modulate BBB tight junction proteins such as claudin 5 (8), full characterisation of the effects of estrogen upon the BBB is lacking, and represents an underexplored aspect of hormonal protection.

We have previously studied the importance of the anti-inflammatory protein annexin A1 (ANXA1) in the BBB, where it plays a major role in the regulation of tight junction expression, contributing to limited barrier permeability (9). Although ANXA1 was originally described as a glucocorticoid second messenger (10), we and others have since reported that it can also be modulated by estrogen (11-13), leading us to hypothesise that estrogen may exert protective effects upon the BBB in inflammation through the regulation of this protein.

Using a combined *in vivo*/*in vitro* approach, we examined the response of the BBB to peripheral inflammatory challenge and the ability of the principal estrogen: estradiol (E2) to restore homeostasis in this system. We report here the presence of sexual dimorphism in the response of the BBB to peripheral pro-inflammatory challenge *in vivo*, and a dual protective role for estradiol upon the inflamed cerebral endothelium *in vitro*, mediated through the regulation of ANXA1 and ICAM-1 expression. Together these actions control movement of both small molecules and immune cells across the cerebral endothelium.

2. Materials and Methods

2.1 Reagents

All reagents are from Sigma-Aldrich (Poole, United Kingdom) unless otherwise stated. Cell culture medium and solutions were purchased from Lonza (Basel, Switzerland). The ERα agonist PPT (4,4',4''-(4-propyl-(5)-pyrazole-1,3,5triyl) trisphenol), the ERβ agonist DPN (2,3-bis(4-Hydroxyphenyl)-propionitrile), the GPR30 agonist G-1 ((±)-1-[(3aR*,4S*,9bS*)-4-(6-bromo-1,3-benzodioxol-5-yl)-3a,4,5,9b-tetrahydro-3H-cyclopenta[c]quinolin-8-yl]-ethanone), the ERβ antagonist PHTPP (4-[2-phenyl-5,7-bis(trifluoromethyl)pyrazolo[1,5-a]pyrimidin-3-yl]phenol) and the GPR30 antagonist G-15 ((3aS*,4R*,9bR*)-4-(6-bromo-1,3-benzodioxol-5-yl)-3a,4,5,9b-3H-cyclopenta[c]quinolone) were purchased from Tocris Bioscience (Bristol, United Kingdom). TNFα and IFNγ were purchased from R&D Systems (Abingdon, United Kingdom).

2.2 Human Recombinant Annexin A1 production and purification

cDNA of human ANXA1 carrying a cleavable N-terminal poly-His tag was expressed in *E. coli*. Recombinant protein was purified on IMAC (GE Healthcare), and the poly-His tag was subsequently removed. Purity of recombinant ANXA1 was confirmed by SDS-PAGE and the 4800 MALDI-TOF/TOF (Applied Biosystems), revealing a 38.6-kDa protein that was >95% pure (9).

2.3 Animal experiments

Male and female 2 and 15 month old C57Bl/6 and AnxA1$^{-/-}$ mice were bred at Charles River under our project QMUL.ES Annexin. Female C57Bl/6 mice were sham-operated or ovariectomised under isofluorane anaesthesia with buprenorphine analgesia, and micro-osmotic pumps containing either estradiol or β-cyclodextrin vehicle were implanted

subcutaneously (Alzet model 2002; Durect Co., Cupertino CA, USA); similar ovariectomy has been previously shown to significantly reduce circulating estrogen in ovariectomised animals when compared with sham-operated mice (14). Mice were sacrificed by exsanguination. All experiments were performed at the same time of day to avoid the confounding effects of circadian rhythm. In some experiments ovariectomised mice were further treated with intravenous (i.v.) human recombinant ANXA1 before further challenge with 3mg/kg lipopolysaccharide (LPS).

2.4 In vivo assessment of BBB leakage

Mice were injected i.p. with 3mg/kg LPS in 100µl saline vehicle and cerebrovascular permeability was assessed at 4 hours, 24 hours or 7 days post-injection. One hour before assessment animals were injected i.v. with 100µl of a 2% (w/v) solution of Evans blue dye in 0.9% saline (Sigma-Aldrich Ltd.; Poole, United Kingdom). Dye was permitted to circulate for 1h before animals were transcardially perfused with 0.9% saline at 4°C to remove circulating dye, as described previously (9); brain Evan's blue content was expressed as µg of dye/mg of brain tissue, normalised to circulating plasma concentrations.

2.5 Murine T lymphocyte transmigration on isolated primary microvascular brain endothelial cells

Murine T cells were isolated from lymph nodes of C57BL/6 WT mice and activated for 3 days in 24-well plates coated with anti-CD3 (1µg/ml) and anti-CD28 (5µg/ml) antibodies (BioLegend), and containing IL-2 (10ng/ml; PeproTech) as previously described (15). Capillaries were extracted from the cortex of 3-month-old WT mice as previously described (9). Isolated vessels were put in culture until confluence. Primary brain microvascular endothelial cells were then used at passage one in 24-well plate Polycarbonate transwell inserts

(surface: 0.33 cm^2, pore size: 5µm; Sigma-Aldrich, UK) and put in contact with murine T lymphocytes for the lymphocyte transmigration assay (4h at 37°C in 5% CO_2) as described in section 2.8.

2.6 hCMEC/D3 cells

The hCMEC/D3 cell line used for *in vitro* and molecular analysis was maintained and treated as described previously (9, 16). For permeability and imaging experiments cells were either polarized through growth on 12-well plate Polyethylene Terephthalate (PET) transwell inserts (surface: 1.12 cm^2, pore size: 0.4 µm; Sigma-Aldrich, UK) coated with calf-skin collagen and fibronectin (Sigma-Aldrich, UK), or plated on Nunc™ Lab-tek Chamber slide system Permanox Plastic 25x75 mm (ThermoScientific, UK).

2.7 In vitro barrier function assessments

Permeability of hCMEC/D3 cell monolayers to 70kDa FITC-dextran (3mg/ml) was measured as described previously (9, 17, 18). Transendothelial electrical resistance (TEER) measurements were performed on 100% confluent cultures using a Millicell-ERS apparatus (Millipore, Watford, United Kingdom) and expressed as $\Omega \bullet cm^2$. Values obtained from cell-free inserts were subtracted from the total values.

2.8 Lymphocyte transmigration assay

hCMEC/D3 brain endothelial cells were cultured in monolayers on 24-well plate Polycarbonate transwell inserts (surface: 0.33 cm^2, pore size: 5µm; Sigma-Aldrich, UK) for 48h prior to assay. After 24h, TNFα and IFNγ (10ng/ml) were added to the upper chambers; after 48h, and just before the assay started, 600µl of complete EGM-2 MV medium was added to the lower compartment. Peripheral blood mononuclear cells (PBMCs), isolated from fresh

venous blood of healthy volunteers by Ficoll-gradient (d=1.077 g/cm^3; Sigma-Aldrich, UK), were added to the upper compartment (1x10^6 in 100 µl) and cells were incubated for 4h at 37°C in 5% CO_2. Inserts were then removed, and the entire volume of the lower compartment was collected to assess transmigrated PBMCs. PBMCs adhering to monolayers were determined by washing inserts with D-PBS once to remove non-bound cells, and then a second time more vigorously with 5mM EDTA in D-PBS (4°C) for 10 minutes. Cells recovered in the EDTA washing step were considered the adherent cell population (19). Adherent and migrated cells were stained with PE-conjugated CD3$^+$ antibody (1:200; eBioscience) and then analysed by flow cytometry to determine relative CD3$^+$ T lymphocyte populations as described below.

2.9 Quantification of ANXA1 by ELISA

Total human ANXA1 was measured by specific sandwich ELISA, as described previously (20).

2.10 Protein extraction and immunoblotting

For ANXA1 analysis the membrane-bound fraction was extracted by EDTA-EGTA wash (1mM in PBS), as previously described (21); total protein extraction was performed by 3 cycles of freeze/thawing in RIPA buffer (1mM EDTA, 150mM NaCl, 50mM Tris·HCl, 1% Triton X-100, 0.1% SDS, 1% sodium deoxycholate, protease inhibitors, pH 7.4). Protein resolution and visualisation was performed as previously described (9, 20, 22), using the following antibodies: Annexin A1 (1:5000; Invitrogen), Ⓟ-S-Annexin A1 [1:1000; (22, 11) and GAPDH (1:5000; Sigma)]. Blots were analysed with NIH Image J 1.42 software.

2.11 Immunofluorescence analysis

hCMEC/D3 cells were cultured on Lab-tek glass slides (Thermo Scientific, UK) pre-coated with rat tail type I collagen (BD Biosciences, San Jose CA, US), following published protocols (9, 23) and using primary antibodies directed against occludin (1:200; Invitrogen) and zonula occludens-1 (ZO-1; 1:100; Invitrogen). Nuclei were counterstained with DAPI. Images were captured by using a TCS SP5 confocal laser scanning microscope (Leica Microsystems) fitted with 405-nm, 488-nm, 594nm and 633-nm lasers, and attached to a Leica DMI6000CS inverted microscope fitted with 63X oil immersion objective lens (NA, 1.4 mm, working distance, 0.17 mm). Images were captured with Leica LAS 2.6.1 software and analysed by using ImageJ software (National Institutes of Healths).

2.12 Flow cytometry

Cells were fixed in 2% (w/v) formaldehyde for 10 minutes at room temperature and then washed and resuspended in D-PBS prior to immunofluorescent profiling, as previously reported (20, 22). Flow cytometric analysis was performed using a BD FACS Fortessa (BD Biosciences); data were analysed using FlowJo software (Treestar Inc, OR, USA).

2.13 shRNA ANXA1 and virus production

Lentiviral vectors (pLKO.1-puro) bearing validated shRNA sequences directed against human ANXA1 (TRC2.0 Mission® shRNA vectors; Sigma-Aldrich, UK) were grown in *E.coli* and purified using Qiagen Miniprep kits (Qiagen Inc, USA) according to manufacturer's instructions. High-titer lentiviral preparations in HEK293T cells and lentiviral infections of hCMEC/D3 endothelial cells were produced as described previously (24). Specific clones were designated as follows: TRCN0000308208 – shRNA A, TRCN0000296381 – shRNA B and TRCN0000296320 – shRNA C. Transduction efficiency and ANXA1 knockdown were verified by western blot analysis as previously reported (25).

2.14 Real-time polymerase chain reaction

RNA was isolated from cells and reverse-transcribed, as described previously (22). Real-time polymerase chain reaction was performed using QuantiTect® SYBR green PCR kit (Qiagen, Crawley, United Kingdom). Primers directed against ANXA1 (QT00078197) and the control genes Rpl32 (QT00046088) and β-actin (QT00095431) coding sequences were purchased from Qiagen (QuantiTect® Primer assay; Qiagen, Crawley, United Kingdom).

2.15 Statistical analysis

Data are expressed as mean ± SEM, with n=3 independent experiments performed in triplicate for *in vitro* studies, and n=8 for *in vivo* analyses. In all cases, normality of distribution was established using the Shapiro-Wilks test, followed by analysis with two-tailed Student's t-tests to compare two groups or for multiple comparison analysis, 1- or 2-way ANOVA followed by Tukey's HSD *post hoc* tests. A p value of less than 5% was considered significant.

2.16 Ethical Approval

All animal experiments were performed in accordance with the UK Animals (Scientific Procedures) Act, 1986. Blood samples from healthy volunteers were collected under St Thomas's Hospital Research Ethics Committee (Ref. 07/Q0702/24) and all volunteers gave written consent before entering the study. The study has followed established SOPs and the experiments were conformed to the principles set out in the WMA Declaration of Helsinki.

2 Results

3.1 Estrogen-dependent sex differences in the BBB response to inflammatory challenge

We initially characterised the response of the murine BBB to a simple systemic inflammatory model, the administration of bacterial lipopolysaccharide (LPS; 3mg/kg i.p.), with assessment of barrier permeability through extravasation of intravenous Evan's blue dye in young adult (2 month) male and female C57Bl/6 mice. A marked sex difference was notable in male animals showing a clear and reproducible, but transient, increase in BBB permeability 4h post-LPS administration, whilst such change was not apparent in females (Fig. 1A). Importantly, however, reproductively senescent female mice (15 month) responded to systemic LPS in a manner analogous to both young and old males, exhibiting significantly enhanced Evan's blue extravasation 4h post-LPS (Fig. 1B).

Given its diverse anti-inflammatory effects (3), estrogen is a major candidate regulator of these differential responses to LPS, hence we investigated the role of this hormone *in vivo*. Young adult female mice (2 month) were ovariectomised and subsequently implanted with osmotic mini-pumps containing either estradiol (E2) or β-cyclodextrin vehicle (26). Ovariectomy with vehicle replacement did not *per se* increase the degree of basal Evans' blue dye extravasation, but in the presence of LPS (3mg/kg body weight i.p. assessed 4h post-injection) it significantly enhanced paracellular permeability (Fig. 1C). Of note, replacement with proestrous levels of estradiol completely prevented this effect (Fig. 1C). Furthermore, 24h pre-treatment with hrANXA1 *via* i.v. [0.6µg/kg body weight; Fig. 1C], (16) mirrored the effect of estradiol (E2) replacement.

3.2 Estradiol regulation of BBB characteristics and lymphocyte migration in vitro

To investigate the cellular and molecular mechanisms behind these *in vivo* responses we utilized the well-established *in vitro* model of immortalised human microvascular endothelial cells, hCMEC/D3 (27). Paracellular permeability of hCMEC/D3 monolayers to 70kDa-FITC dextran was significantly enhanced by 24h stimulation with TNFα and IFNγ (10ng/ml 24h; Fig. 2A), an effect markedly attenuated by treatment for the last 8h with estradiol (100nM), previously selected as optimal dose and time response (Suppl. Fig.1). Similarly, trans-endothelial electrical resistance of hCMEC/D3 monolayers was significantly reduced by TNFα and IFNγ treatment, an effect reversed by estradiol exposure (Fig. 2B). Inter-endothelial tight junctions are the principal effectors of the maintenance of the paracellular permeability barrier and trans-endothelial resistance; hence we examined the ability of estradiol to modulate two of the component proteins of these structures, occludin and zonula occludens-1 (ZO-1). Treatment of polarised hCMEC/D3 monolayers grown on transwell filters with TNFα and IFNγ (10ng/ml, 24h) induced a clear loss of marginal occludin and ZO-1 immunofluorescence, an effect reversed by treatment with estradiol (100nM, last 8h; Fig. 2C-D). Together, these data provide evidence that inflammation-induced changes in endothelial cell interactions can be countered by estradiol, providing a molecular counterpart to the changes seen in the whole animal system.

A major function of the BBB is the regulation of immune cells migration from the circulation into the brain parenchyma. To model the effects of estradiol upon this parameter, we studied the interaction of human peripheral blood lymphocytes with polarised hCMEC/D3 monolayers grown on transwell filters. Inflammatory stimulation (TNFα + IFNγ, 10ng/ml, 24h) of hCMEC/D3 cells significantly enhanced numbers of both adherent and transmigrated $CD3^+$ lymphocytes, a phenomenon markedly inhibited by pre-treatment of the hCMEC/D3 cells with estradiol (100nM, last 8h; Fig. 3A-B). Similar results were obtained using primary murine cerebromicrovascular endothelia and T cells (Suppl. Fig. 2). Correlating with these changes in

lymphocyte migration, endothelial surface expression of ICAM-1, a cell adhesion molecule that is critically required for efficient lymphocyte transmigration (28), was significantly enhanced by cytokine stimulation, an effect attenuated by a similar estradiol pre-treatment (Fig. 3C).

3.3 Estradiol actions are mediated through the BBB regulator ANXA1

Previously, we described the critical role played by ANXA1 in governing BBB integrity, promoting tight junction formation and consequently enhancing inter-endothelial tightness (9). As we and others have shown this protein to be transcriptionally modulated by estrogen (11-13), we investigated the possibility that regulation of ANXA1 underlies the protective effects of estradiol upon the BBB (see also Fig.1C). Characterisation of brain microvascular capillary ANXA1 content revealed a clear female-dominant sex difference in vessels from young (2 month) wild-type mice, but also indicated that female vessel ANXA1 expression dramatically declined between 2 and 15 month of age (Fig. 4A). Importantly, removal of circulating estrogen by ovariectomy significantly lowered cerebral microvascular ANXA1, an effect reversed upon estradiol replacement (Fig. 4B). Together, these findings suggest that the effects of aging were due at least in part to the reproductive senescence-associated decline in estrogen seen in mice (29).

We used an immunoneutralisation strategy (20) to examine the role of ANXA1 in mediating the protective effects of estradiol, assessing hCMEC/D3 paracellular permeability. Inclusion of an anti-ANXA1 antibody had no effect on TNFα/IFNγ induced paracellular permeability, but it was able to block estradiol-induced reversal of this permeability change, an effect not seen by addition of the relevant IgG_{2A} isotype control (Fig. 4C). Confirming the position of ANXA1 as a mediator of estradiol effects, hCMEC/D3 cells stably transduced with lentivirus-

borne shRNA sequences targeting ANXA1 (Suppl. Fig. 3) displayed enhanced basal paracellular permeability, as shown previously (9). Notably, estradiol was not able to prevent the additional increase in permeability seen with TNFα/IFNγ treatment of these cells (Fig. 4D). To investigate the contribution of ANXA1 to the control of lymphocyte migration by estradiol we first studied the adhesion to and migration across hCMEC/D3 monolayers under-expressing ANXA1 (shRNA clones) of human peripheral blood $CD3^+$ lymphocytes. As expected the reduction in ANXA1 expression impeded the actions of estrogen in reverting the effects of TNFα/IFNγ upon the endothelium (Fig 4E, F). Furthermore, lower expression of ANXA1 *per se* enhanced the impact of TNFα/IFNγ upon ICAM-1 on hCMEC/D3 cells, and moreover prevented the modulatory effects of estrogen upon this expression (Fig. 4G). These data strongly indicate that the protective actions of estrogen against inflammation-induced BBB damage are mediated through modulation of ANXA1 expression. Final validation of the role of ANXA1 in the BBB protective effects of estradiol was given through study of sex differences in cerebrovascular permeability in ANXA1 null mice (30). As expected, ANXA1 null mice showed markedly higher basal Evans' blue extravasation than wild-type animals, although surprisingly this was not further raised by treatment with LPS (3mg/kg i.p.); importantly however, no signs of sex differences were apparent in any treatment groups (Fig 4H).

3.4 Receptor-specific roles for ERβ and GPR30 in mediating estrogen actions on the BBB

To further investigate the mechanisms whereby estradiol could exert these protective effects, we examined the potential role of the three main estrogen receptors ERα, ERβ and the G protein coupled estrogen receptor GPR30; expression of all three being detectable on hCMEC/D3 cells by flow cytometry (Fig. 5A). Using selective estrogen receptor ligands, we assessed the relative involvement of the different estrogen receptors in ANXA1 regulation, analysing the

membrane-bound pool known to be reflective of secreted ANXA1 (22), and the total intracellular pool. Estradiol treatment significantly enhanced membrane-bound ANXA1, an effect replicated by the GPR30 agonist G1, but not by either the ERα agonist PPT or the ERβ agonist DPN (Fig. 5B). Intriguingly, application of either the ERβ antagonist PHTPP or the GPR30 antagonist G15 prevented estradiol-induced up-regulation of membrane-bound ANXA1 (Fig. 5B). In contrast, treatment of hCMEC/D3 cells with estradiol or DPN, but neither PPT nor G1, increased intracellular ANXA1 content, an effect blocked by PHTPP but not G15 (Fig. 5C) indicating a role for ERβ in increasing the intracellular pool of ANXA1. Confirming that changes in intracellular ANXA1 content were due to *de novo* synthesis rather than secretory block, qRT-PCR analysis of ANXA1 mRNA revealed that either estradiol or DPN, but not G1, significantly enhanced ANXA1 mRNA levels, an effect inhibited by PHTPP but not G15 (Fig. 5D-E). We have previously shown the importance of ANXA1 N-terminal serine phosphorylation for the export and activity of this protein (22) hence we investigated whether stimulation of hCMEC/D3 cells with estradiol resulted in serine phosphorylation. Whilst estradiol did not appear to induce significant changes in the degree of N-terminal serine phosphorylation in cytoplasmic ANXA1, stimulation of hCMEC/D3 cells with the hormone induced both rapid (2 minutes) and delayed (8h) phosphorylation of cell surface associated ANXA1 (Fig. 5F). Together, these experiments indicate dual, receptor-specific actions of estradiol upon ANXA1, namely, the stimulation of protein synthesis via ERβ and the induction of N-terminal phosphorylation and subsequent membrane externalisation through GPR30.

We made similar use of estrogen receptor antagonists to define the relative roles of ERβ and GPR30 in mediating the regulatory effect of estradiol upon lymphocyte migration. Pre-incubation of hCMEC/D3 cells with the ERβ antagonist PHTPP completely prevented estradiol from reversing TNFα/IFNγ induced $CD3^+$ lymphocyte adhesion (Fig 6A) and transmigration

(Fig 6C). Moreover, pre-treatment with the GPR30 antagonist G15 did not modulate the effects of estradiol on either lymphocyte adhesion (Fig. 6B) or transmigration (Fig. 6D). We then investigated whether blockade of estrogen receptors similarly affected ICAM-1 expression, revealing that PHTPP, but not G15, reversed the effects of estradiol upon TNFα/IFNγ-induced ICAM-1 up-regulation (Fig. 6E-F), confirming a central role for ERβ in this action.

3 Discussion

Steroid hormones have long been known to possess anti-inflammatory properties, indeed synthetic glucocorticoid receptor agonists are amongst the most clinically potent anti-inflammatory drugs available, but it is only relatively recently that the anti-inflammatory potential of estrogen has begun to be closely studied (3). The primary interface between the CNS and the inflammatory response, the BBB, has been examined as a target for estrogen action (8, 26, 31, 32), but understanding of the molecular pathways governing hormonal influence is lacking. Here, we reveal parallel protective effects of estrogen upon the BBB, preventing inflammation-induced tight junction breakdown through enhancement of ANXA1 expression and limiting lymphocyte migration by modulation of endothelial cell ICAM-1. Moreover, we reveal for the first time the estrogen receptor subtypes involved in mediating these actions, delineating independent but complementary roles for ERβ and GPR30.

An important feature of the current study is that the protective effects of estrogen upon the BBB were only discernible in the presence of inflammatory stimuli. In this, estrogen seems to act primarily as a homeostatic signal, limiting disturbance and restoring balanced function to the BBB, and can thus be truly considered a protective agent. This protective aspect of estrogen may go some way to explaining the well-known sex differences in the incidence of major cerebrovascular disease, most notably stroke (33, 34), differences that markedly diminish past the age of menopause and the associated decline in circulating estrogen (35). Moreover, many of the most important risk factors for stroke are inflammatory conditions, e.g. atherosclerosis, diabetes, obesity, and it is increasingly evident that the associated high levels of circulating cytokines enhance BBB vulnerability, directly contributing to increased stroke risk (36). Our finding that the protective effects of estrogen upon the BBB are most apparent following

inflammatory challenge may thus at least partly underlie its protective effects in pre-menopausal women.

In addition to bolstering the evidence for ANXA1 as an estrogen mediator, the current study provides the first description of the molecular mechanism whereby these agents interact. The primary function of the BBB is to shield the CNS from harmful challenges (37), of which inflammatory mediators are an acute example. Our studies thus extend the local pro-resolving actions of ANXA1 (38) to the brain, underlining its wider physiological involvement in the response to inflammation. Additionally, we have identified a dual, receptor-specific action of estrogen upon ANXA1, increasing synthesis *via* ERβ and modulating ANXA1 post-translational modification *via* GPR30. Phosphorylation of ANXA1 is critically required for its extracellular export and consequent actions (22), and, whilst identification of the kinase(s) responsible lies beyond the scope of this study, suspicion falls upon members of the PKC family, as these enzymes are both activated following GPR30 stimulation (39) and can phosphorylate ANXA1 (21, 22, 40, 41).

In studying the role of ANXA1 as a mediator of estrogen action, we have also identified a clear role for the GPR30 in maintaining BBB integrity under challenge. This receptor is known to be expressed on the cerebrovascular endothelium *in vivo* (42, 43), but as yet evidence for its function remains thin. Our data place GPR30 at the centre of the mechanisms responsible for preserving the BBB permeability barrier during inflammatory challenge. Moreover, as GPR30 is a G protein coupled receptor, and thus is activated much more rapidly than the classical estrogen receptors ERα and ERβ, it represents a mechanism whereby estrogen can swiftly protect the cerebral vasculature following inflammation.

The interaction between ANXA1 and estrogen is a major pathway by which the hormone can exert an anti-inflammatory, protective effect upon the BBB, affecting not only paracellular permeability of circulating molecules but also regulating emigration of lymphocytes into the brain. This result is of significance as it represents the first mechanistic explanation of how estrogen can limit inflammation-induced cell entry into the brain parenchyma. Lymphocyte entry into the brain tissue itself remains a controversial topic, with debate centering on whether cells truly pass the glia limitans and interact with neurones directly, or whether they remain in the perivascular space (44). Regardless, it is clear that extravasated lymphocytes have the potential to sustain or even initiate inflammatory reactions *in situ* (45), which, given the high vulnerability of neurones to inflammatory challenge, poses significant risks for brain tissue integrity. Estrogen, through its ability to suppress inflammation-induced endothelial ICAM-1 upregulation can clearly attenuate lymphocyte migration, further shielding the brain parenchyma from peripheral inflammatory insult. Previous studies have indicated a role for ERβ in the actions of estrogen on ICAM-1 expression in salivary gland epithelial cells (46) and arterial smooth muscle (47), but for the first time we not only extend these findings to the endothelial cells of the cerebral vasculature, but provide a clear definition of the next step in the pathway downstream of ERβ, namely ANXA1. The question as to how ANXA1 regulates ICAM-1 expression requires further study, but may involve an interaction with signalling molecules such as AMPK or PPARα (48).

Taken together, our data propose a mechanism of action for estrogen and ANXA1 in the modulation of BBB tightness and lymphocyte migration as schematized in figure 7: 1) estradiol *via* GPR30 induces the post-transcriptional modification of ANXA1, which is known to lead to its export and consequent autocrine/paracrine induction of BBB tightness pathways; 2) estradiol through ERβ blocks lymphocyte adhesion and migration by regulating ICAM-1

expression through ANXA1. These combined mechanisms may work together in regulating immune cells entry into the brain parenchyma.

In conclusion, our findings identify novel, anti-inflammatory actions of estrogen upon the BBB, namely the regulation of inter-endothelial cell permeability and the limitation of lymphocyte transmigration. Intriguingly, whilst these two actions appear to be governed in the main by different estrogen receptors, with GPR30 regulating paracellular permeability and ERβ limiting lymphocyte migration through suppression of ICAM-1 expression, these actions are both mediated by the downstream protein ANXA1, highlighting the significance of this protein in the BBB. Together, these harmonizing pathways represent clear mechanisms through which estrogen can aid the maintenance of BBB homeostasis in the face of inflammatory challenge.

4 Conclusions

The prevalence of inflammatory cerebrovascular diseases shows a distinct male predominance, with numerous studies showing women to be relatively protected. Understanding why this is the case remains a challenge. Here, we identify a powerful protective action of the female sex steroid estrogen, showing that this hormone can both enhance inter-endothelial cell tight junction function and limit lymphocyte extravasation following challenge with inflammatory cytokines. Moreover, we identify these actions as being mediated through upregulation of the potent anti-inflammatory and blood-brain barrier regulating protein annexin A1. Together our data offer a novel mechanism whereby estrogen can protect the brain from insult, and suggest an innovative pathway for therapeutic targeting in cerebrovascular disease.

Author contributions

Elisa Maggioli: Performed *in vivo* and in vitro experiments, data analysis.

Simon McArthur: Performed *in vivo* work, the immunocytochemical and confocal microscopic analysis, qPCR, data analysis, contributed to writing and discussion of the manuscript.

Claudio Mauro: Performed shRNA lentivirus production and contributed to discussion of the manuscript.

Julius Kieswich: Animal handling and support in vivo experiments.

Dennis Kusters: Performed ANXA1 expression and purification.

Chris Reutelingsperger: Provided ANXA1 recombinant protein.

Magdi Yaqoob: Contributed to discussion and write up of the manuscript.

Egle Solito: PI of the project, performed experiments, data analysis, writing and discussion of the manuscript.

Financial interest

The authors declare no conflict of interests.

Acknowledgment

This work was supported by ARUK –PPG2013B-2 and FISM-3/15/F14 to ES, Barts and the London Trust to MY, and British Heart Foundation Fellowship FS/12/38/29640 to CM.

References

1. Gillies GE & McArthur S (2010) Estrogen actions in the brain and the basis for differential action in men and women: a case for sex-specific medicines. *Pharmacol Rev* 62(2):155-198.
2. Czlonkowska A, Ciesielska A, Gromadzka G, & Kurkowska-Jastrzebska I (2005) Estrogen and cytokines production - the possible cause of gender differences in neurological diseases. *Curr Pharm Des* 11(8):1017-1030.
3. Nadkarni S & McArthur S (2013) Oestrogen and immunomodulation: new mechanisms that impact on peripheral and central immunity. *Curr Opin Pharmacol* 13(4):576-581.
4. Carvey PM, Hendey B, & Monahan AJ (2009) The blood-brain barrier in neurodegenerative disease: a rhetorical perspective. *J Neurochem* 111(2):291-314.
5. Cignarella A, *et al.* (2009) Distinct roles of estrogen receptor-alpha and beta in the modulation of vascular inducible nitric-oxide synthase in diabetes. *J Pharmacol Exp Ther* 328(1):174-182.
6. Gameiro CM, Romao F, & Castelo-Branco C (2010) Menopause and aging: changes in the immune system--a review. *Maturitas* 67(4):316-320.
7. Dietrich JB (2004) Endothelial cells of the blood-brain barrier: a target for glucocorticoids and estrogens? *Front Biosci* 9:684-693.
8. Burek M, Steinberg K, & Forster CY (2014) Mechanisms of transcriptional activation of the mouse claudin-5 promoter by estrogen receptor alpha and beta. *Mol Cell Endocrinol* 392(1-2):144-151.
9. Cristante E, *et al.* (2013) Feature Article: Identification of an essential endogenous regulator of blood-brain barrier integrity, and its pathological and therapeutic implications. *Proc Natl Acad Sci U S A* 110(3):832-841.

10. Flower RJ & Blackwell GJ (1979) Anti-inflammatory steroids induce biosynthesis of a phospholipase A2 inhibitor which prevents prostaglandin generation. *Nature* 278(5703):456-459.

11. Solito E, Froud K, Christian H, Morris J, & Buckingham J (2003) Opposite effects of dexamethasone and oestardiol on annexin 1 expression. *Endocrine Abstracts* Endocrine Abstracts:65.

12. Davies E, Omer S, Morris JF, & Christian HC (2007) The influence of 17beta-estradiol on annexin 1 expression in the anterior pituitary of the female rat and in a folliculo-stellate cell line. *J Endocrinol* 192(2):429-442.

13. Nadkarni S, Cooper D, Brancaleone V, Bena S, & Perretti M (2011) Activation of the annexin A1 pathway underlies the protective effects exerted by estrogen in polymorphonuclear leukocytes. *Arterioscler Thromb Vasc Biol* 31(11):2749-2759.

14. Villar IC, *et al.* (2011) Suppression of endothelial P-selectin expression contributes to reduced cell trafficking in females: an effect independent of NO and prostacyclin. *Arterioscler Thromb Vasc Biol* 31(5):1075-1083.

15. Haas R, *et al.* (2015) Lactate Regulates Metabolic and Pro-inflammatory Circuits in Control of T Cell Migration and Effector Functions. *PLoS Biol* 13(7):e1002202.

16. Weksler BB, *et al.* (2005) Blood-brain barrier-specific properties of a human adult brain endothelial cell line. *FASEB J* 19(13):1872-1874.

17. Abbott NJ, Hughes CC, Revest PA, & Greenwood J (1992) Development and characterisation of a rat brain capillary endothelial culture: towards an in vitro blood-brain barrier. *J Cell Sci* 103 (Pt 1):23-37.

18. Coisne C, *et al.* (2005) Mouse syngenic in vitro blood-brain barrier model: a new tool to examine inflammatory events in cerebral endothelium. *Lab Invest* 85(6):734-746.

19. Rohnelt RK, Hoch G, Reiss Y, & Engelhardt B (1997) Immunosurveillance modelled in vitro: naive and memory T cells spontaneously migrate across unstimulated microvascular endothelium. *Int Immunol* 9(3):435-450.

20. McArthur S, *et al.* (2010) Annexin A1: a central player in the anti-inflammatory and neuroprotective role of microglia. *J Immunol* 185(10):6317-6328.

21. Solito E, *et al.* (2006) Post-translational modification plays an essential role in the translocation of annexin A1 from the cytoplasm to the cell surface. *FASEB J* 20(9):1498-1500.

22. McArthur S, *et al.* (2009) Annexin A1 regulates hormone exocytosis through a mechanism involving actin reorganization. *FASEB J* 23(11):4000-4010.

23. Lopez-Ramirez MA, *et al.* (2012) Role of Caspases in Cytokine-Induced Barrier Breakdown in Human Brain Endothelial Cells. *J Immunol*.

24. Rubinson DA, *et al.* (2003) A lentivirus-based system to functionally silence genes in primary mammalian cells, stem cells and transgenic mice by RNA interference. *Nat Genet* 33(3):401-406.

25. Solito E, Raguenes-Nicol C, de Coupade C, Bisagni-Faure A, & Russo-Marie F (1998) U937 cells deprived of endogenous annexin 1 demonstrate an increased PLA2 activity. *Br J Pharmacol* 124(8):1675-1683.

26. Burek M, Arias-Loza PA, Roewer N, & Forster CY (2010) Claudin-5 as a novel estrogen target in vascular endothelium. *Arterioscler Thromb Vasc Biol* 30(2):298-304.

27. Weksler B (2005) Linking thrombophilia and idiopathic intracranial hypertension. *J Lab Clin Med* 145(2):63-64.

28. Herter J & Zarbock A (2013) Integrin Regulation during Leukocyte Recruitment. *J Immunol* 190(9):4451-4457.

29. Parkening TA, Lau IF, Saksena SK, & Chang MC (1978) Circulating plasma levels of pregnenolone, progesterone, estrogen, luteinizing hormone, and follicle stimulating hormone in young and aged C57BL/6 mice during various stages of pregnancy. *J Gerontol* 33(2):191-196.

30. Hannon R, *et al.* (2003) Aberrant inflammation and resistance to glucocorticoids in annexin 1-/- mouse. *FASEB J* 17(2):253-255.

31. Suzuki S, Brown CM, & Wise PM (2006) Mechanisms of neuroprotection by estrogen. *Endocrine* 29(2):209-215.

32. Oztas B, Kucuk M, & Kaya M (2001) Sex-dependent changes in blood-brain barrier permeability in epileptic rats following acute hyperosmotic exposure. *Pharmacol Res* 43(5):469-472.

33. Suzuki S, Brown CM, & Wise PM (2009) Neuroprotective effects of estrogens following ischemic stroke. *Front Neuroendocrinol* 30(2):201-211.

34. Koellhoffer EC & McCullough LD (2013) The effects of estrogen in ischemic stroke. *Transl Stroke Res* 4(4):390-401.

35. Haast RA, Gustafson DR, & Kiliaan AJ (2012) Sex differences in stroke. *J Cereb Blood Flow Metab* 32(12):2100-2107.

36. Murray KN, Buggey HF, Denes A, & Allan SM (2013) Systemic immune activation shapes stroke outcome. *Mol Cell Neurosci* 53:14-25.

37. Abbott NJ, Patabendige AA, Dolman DE, Yusof SR, & Begley DJ (2010) Structure and function of the blood-brain barrier. *Neurobiol Dis* 37(1):13-25.

38. Perretti M & D'Acquisto F (2009) Annexin A1 and glucocorticoids as effectors of the resolution of inflammation. *Nat Rev Immunol* 9(1):62-70.

39. Li T, *et al.* (2014) Age and sex differences in vascular responsiveness in healthy and trauma patients: contribution of estrogen receptor-mediated Rho kinase and PKC pathways. *Am J Physiol Heart Circ Physiol* 306(8):H1105-1115.

40. Solito E, *et al.* (2003) Dexamethasone induces rapid serine-phosphorylation and membrane translocation of annexin 1 in a human folliculostellate cell line via a novel nongenomic mechanism involving the glucocorticoid receptor, protein kinase C, phosphatidylinositol 3-kinase, and mitogen-activated protein kinase. *Endocrinology* 144(4):1164-1174.

41. Yazid S, *et al.* (2010) Anti-allergic drugs and the Annexin-A1 system. *Pharmacol Rep* 62(3):511-517.

42. Broughton BR, *et al.* (2013) Stroke increases g protein-coupled estrogen receptor expression in the brain of male but not female mice. *Neurosignals* 21(3-4):229-239.

43. Tu J & Jufri NF (2013) Estrogen signaling through estrogen receptor beta and G-protein-coupled estrogen receptor 1 in human cerebral vascular endothelial cells: implications for cerebral aneurysms. *Biomed Res Int* 2013:524324.

44. Ransohoff RM & Engelhardt B (2012) The anatomical and cellular basis of immune surveillance in the central nervous system. *Nat Rev Immunol* 12(9):623-635.

45. Gee JM, Kalil A, Shea C, & Becker KJ (2007) Lymphocytes: potential mediators of postischemic injury and neuroprotection. *Stroke* 38(2 Suppl):783-788.

46. Tsinti M, *et al.* (2009) Functional estrogen receptors alpha and beta are expressed in normal human salivary gland epithelium and apparently mediate immunomodulatory effects. *Eur J Oral Sci* 117(5):498-505.

47. Xing D, *et al.* (2007) Estrogen modulates TNF-alpha-induced inflammatory responses in rat aortic smooth muscle cells through estrogen receptor-beta activation. *Am J Physiol Heart Circ Physiol* 292(6):H2607-2612.

48. Hou X & Pei F (2015) Estradiol Inhibits Cytokine-Induced Expression of VCAM-1 and ICAM-1 in Cultured Human Endothelial Cells Via AMPK/PPARalpha Activation. *Cell Biochem Biophys*.

Figure Legends

Figure 1 Estradiol protects against inflammation-induced BBB integrity defects. **A** Extravasation of Evan's blue dye into brain parenchyma over a one hour period in two month old male and female C57Bl/6 mice (n=8) following i.p. injection of saline or LPS (3mg/kg body weight) for 4h, 24h or 7 days, data are mean ± SEM, *p<0.05 *vs.* same sex saline control. **B** Extravasation of Evan's blue dye into brain parenchyma over a one hour period in young (2 month) and old (15 month) male and female C57Bl/6 mice (n=8) 4h following i.p. injection of LPS (3 mg/kg body weight) or 100µl saline vehicle.; data are expressed as mean ± SEM, *p<0.05 *vs.* 2 month, same sex saline control. **C** Extravasation of Evan's blue dye into the brain parenchyma over a three hour period in sham operated or ovariectomised female C57Bl/6 mice (2 month; n=8) receiving 14 days treatment with either estradiol (2µg/kg/day) or β-cyclodextrin, or receiving a single i.v. injection of hrANXA1 (0.6µg/kg); data are mean ± SEM, *p<0.05 *vs.* saline control, +p<0.05 *vs.* OVX-vehicle treated.

Figure 2 Estradiol prevents cytokine-induced disruption of BBB endothelial permeability characteristics and tight junction component subcellular distribution. A Assessment of the paracellular permeability of hCMEC/D3 monolayers to 70kDa FITC-dextran following treatment for 24h with TNFα + IFNγ (both 10ng/ml), with or without inclusion of 100nM estradiol for the last 8 hours of incubation; data are mean ± SEM, n=3 (three independent experiments performed each in triplicate), *p<0.05 *vs.* unstimulated control, +p<0.05 *vs.* TNFα/IFNγ treatment control. **B** Trans-endothelial electrical resistance of hCMEC/D3 monolayers following treatment for 24h with TNFα + IFNγ (both 10ng/ml), with or without inclusion of 100nM estradiol for the last 8 hours of incubation; data are mean ± SEM, n=3 (three independent experiments performed each in triplicate), *p<0.05 *vs.* unstimulated control,

+p<0.05 *vs.* TNFα/IFNγ treatment control **C** Representative confocal microscopic analysis of hCMEC/D3 monolayer occludin expression following treatment for 24h with TNFα + IFNγ (both 10ng/ml), with or without inclusion of 100nM estradiol for the last 8 hours of incubation; arrowheads indicate the presence or absence of peripheral occludin staining with different treatments; data are representative of three independent experiments. **D** Confocal microscopic analysis of hCMEC/D3 monolayer ZO-1 expression following treatment for 24h with TNFα + IFNγ (both 10ng/ml), with or without inclusion of 100nM estradiol for the last 8 hours of incubation; arrowheads indicate the presence or absence of peripheral ZO-1 staining with different treatments; data are representative of three independent experiments.

Figure 3 Estradiol prevents peripheral blood lymphocyte migration across an inflamed endothelium and prevents inflammatory cytokines induced up-regulation of ICAM-1. A Adhesion of $CD3^+$ lymphocytes to hCMEC/D3 monolayers following treatment with TNFα + IFNγ (both 10ng/ml) and/or estradiol (100nM). Data are mean ± SEM, n=3 (three independent experiments performed each in triplicate), *p<0.05 *vs.* unstimulated control, +p<0.05 *vs.* TNFα/IFNγ treatment alone. **B** Transmigration of $CD3^+$ lymphocytes across hCMEC/D3 monolayers following treatment with TNFα + IFNγ (both 10ng/ml) and/or estradiol (100nM). Data are mean ± SEM, n=3 (three independent experiments performed each in triplicate), *p<0.05 *vs.* unstimulated control, +p<0.05 *vs.* TNFα/IFNγ treatment alone. **C** Expression of ICAM-1 on the cell surface of hCMEC/D3 monolayers following treatment with TNFα + IFNγ (both 10ng/ml) and/or estradiol (100nM) data are mean ± SEM, n=3 (three independent experiments performed each in triplicate), *p<0.05 *vs.* unstimulated control, +p<0.05 *vs.* TNFα/IFNγ treatment alone.

Figure 4 Protection of BBB integrity by estradiol is dependent upon the tight junction regulator ANXA1. A Expression of ANXA1 in cerebral capillary endothelia from male (2 month) and female (2 and 15 month) C57Bl/6 mice assessed by western blot; data are mean ± SEM, n=8, *p<0.05 *vs.* male, +p<0.05 *vs.* young female. **B** Expression of ANXA1 in cerebral capillary endothelia from ovariectomised C57Bl/6 mice treated with PEG-400 vehicle or estradiol (2µg/kg/day) assessed by western blot; data are mean ± SEM, n=8, *p<0.05 *vs.* OVX + vehicle, +p<0.05 *vs.* OVX + E2. **C** Inclusion of a neutralizing anti-ANXA1 antibody, but not its IgG_{2A} control, blocks the ability of estradiol to reverse the cytokine-induced enhancement of paracellular permeability; data are mean ± SEM, n=3 (three independent experiments performed each in triplicate), *p<0.05 *vs.* unstimulated cells. **D** Stable infection of hCMEC/D3 cells with an shRNA-lentivirus construct targeting ANXA1 limits the ability of estradiol to reverse TNFα/IFNγ-induced paracellular permeability; data are mean ± SEM, n=3 (independent experiments performed each in triplicate), *p<0.05 *vs.* unstimulated cells, +p<0.05 *vs.* TNFα/IFNγ alone. **E-F** Adherent (E) and transmigrated (F) $CD3^+$ lymphocytes following 4h co-incubation of human PBMCs and hCMEC/D3 monolayers stably infected with an shRNA construct targeting ANXA1, previously treated for 24h with TNFα + IFNγ (both 10ng/ml), with or without inclusion of 100nM estradiol for the last 8 hours of incubation; data are mean ± SEM, n=3 (three independent experiments performed each in triplicate), *p<0.05 *vs.* unstimulated control, +p<0.05 *vs.* TNFα/IFNγ treatment alone. **G** Stable infection of hCMEC/D3 cells with an shRNA construct targeting ANXA1 affected the ability of estradiol to reverse TNFα/IFNγ-induced increases in cell surface ICAM-1 expression; data are mean ± SEM, n=3 (three independent experiments performed each in triplicate), *p<0.05 *vs.* unstimulated cells, +p<0.05 *vs.* TNFα/IFNγ alone. **H** Extravasation of Evan's blue dye into brain parenchyma over a one hour period in two month old male and female *AnxA1*$^{-/-}$ mice

(n=8) following i.p. injection of saline or LPS (3mg/kg body weight) for 4h, 24h or 7 days, data are mean ± SEM.

Figure 5 Estradiol promotes ANXA1 production *via* ERβ and export *via* GPR30. A Flow cytometry analysis of ERα, ERβ and GPR30 expression in hCMEC/D3 cells; histograms are composed of 10000 events. **B** Membrane-bound ANXA1, measured by ELISA, from hCMEC/D3 monolayers treated for 8h with the estrogen receptor agonists Estradiol (E2, 100nM), PPT (200pM), DPN (850pM) or G1 (2nM) or with a combination of the estrogen receptor antagonists PHTPP (140nM) or G15 (20nM) with estradiol (E2, 100nM); data are mean ± SEM, n=3 (three independent experiments performed each in triplicate), *p<0.05 *vs.* untreated cells, +p<0.05 *vs.* cells treated with estradiol alone. **C** Intracellular ANXA1 in hCMEC/D3 monolayers treated for 8h with the estrogen receptor agonists estradiol (100nM), PPT (200pM), DPN (850pM) or G1 (2nM) or with a combination of the estrogen receptor antagonists PHTPP (140nM) or G15 (20nM) with estradiol (100nM); data are mean + SEM, n=3 (three independent experiments performed each in triplicate), *p<0.05 *vs.* untreated cells, +p<0.05 *vs.* cells treated with estradiol alone. **D** Quantitative RT-PCR analysis of *ANXA1* mRNA expression (corrected to the housekeeping gene Rpl32) in hCMEC/D3 monolayers treated for 8h with estradiol (100nM), DPN (850pM) or G1 (2nM); data are mean ± SEM, n=3 (three independent experiments performed each in triplicate) *p<0.05 *vs.* untreated cells. **E** Quantitative RT-PCR analysis of *ANXA1* mRNA expression in hCMEC/D3 monolayers treated for 8h with estradiol (100nM), with or without pre-treatment for 30 minutes with the estrogen receptor antagonists PHTPP (140nM) or G15 (20nM); data are mean ± SEM, n=3 (three independent experiment performed each in triplicate), *p<0.05 *vs.* untreated cells. **F** Typical western blot analysis of total and N-terminal serine-phosphorylated ANXA1 content in intracellular and membrane fractions of hCMEC/D3 monolayers treated for 0, 2, 5, 10 or 30

minutes or 8 hours with 100nM estradiol, alongside GAPDH loading controls; presented blots are representative of 3 independent experiments.

Figure 6 Estradiol regulates $CD3^+$ lymphocyte adhesion and migration and ICAM-1 expression *via* ERβ. A Pre-incubation of hCMEC/D3 monolayers with the ERβ antagonist PHTPP prevents the reversal of TNFα/IFNγ-induced $CD3^+$ lymphocyte adhesion afforded by incubation with estradiol in untreated cells; data are mean ± SEM, n=3 (three independent experiments performed each in triplicate), *p<0.05 *vs.* control, +p<0.05 vs. TNFα/INFγ treatment alone. **B** Pre-incubation of hCMEC/D3 monolayers with the GPR30 antagonist G15 did not change how estradiol affected $CD3^+$ lymphocyte adhesion induced by TNFα/INFγ; data are mean ± SEM, n=3 (three independent experiments performed each in triplicate), *p<0.05 *vs.* control, +p<0.05 *vs.* TNFα/IFNγ treatment alone. **C** Pre-incubation of hCMEC/D3 monolayers with the ERβ antagonist PHTPP prevented the reversal of TNFα/IFNγ-induced $CD3^+$ lymphocyte transmigration afforded by incubation with estradiol in untreated cells, data are mean ± SEM, n=3 (three independent experiments performed each in triplicate), *p<0.05 *vs.* control, +p<0.05 *vs.* TNFα/IFNγ treatment alone. **D** Pre-incubation of hCMEC/D3 monolayers with the GPR30 antagonist G15 did not affect the reversal of TNFα/IFNγ-induced $CD3^+$ lymphocyte transmigration afforded by incubation with estradiol, data are mean ± SEM, n=3 (three independent experiments performed each in triplicate), *p<0.05 *vs.* control, +p<0.05 *vs.* TNFα/IFNγ treatment alone. **E** Pre-incubation of hCMEC/D3 monolayers with the ERβ antagonist PHTPP inhibited the reversal of TNFα/IFNγ-induced cell surface ICAM-1 up-regulation afforded by incubation of untreated cells with estradiol, data are mean ± SEM, n=3 (three independent experiments performed each in triplicate), *p<0.05 *vs.* control, +p<0.05 *vs.* TNFα/IFNγ treatment alone. **F** Pre-incubation of hCMEC/D3 monolayers with the GPR30 antagonist G15 did not affect the reversal of TNFα/IFNγ-induced cell surface ICAM-1 up-

regulation afforded by incubation with estradiol, data are mean ± SEM, n=3 (three independent experiments each performed in triplicate), *p<0.05 *vs.* control, +p<0.05 *vs.* TNFα/IFNγ treatment alone.

Figure 7 Schematic representations of potential mechanisms of action of Estradiol in protecting the brain against neuroinflammation. 1) Estradiol binds to its membrane-bound receptor GPR30 promoting ANXA1 phosphorylation. Once phosphorylated, ANXA1 can bind to its specific receptor FPR2 (as shown in (9)) and enhance the stabilization of tight junctions via modulation of the actin cytoskeleton. 2) Under inflammatory conditions, estradiol binds to its nuclear receptor ERβ enhancing ANXA1 transcription, which can then trigger a down-modulation of ICAM-1 expression. As ICAM-1 is necessary for endothelium-leukocyte interplay, reduced expression attenuates leukocyte adhesion and transmigration.

Supplemental Figure 1 Estradiol promotes hCMEC/D3 cell ANXA1 production in a dose- and time-dependent manner. A Total cellular ANXA1 content in hCMEC/D3 monolayers incubated with increasing concentrations of estradiol for 8 hours; data are mean ± SEM, n=3 (three independent experiments performed each in triplicate) , *p<0.05 vs. untreated cells. **B** Total cellular ANXA1 content in hCMEC/D3 monolayers incubated with 100nM estradiol for increasing periods of time; data are mean ± SEM, n= 3 (three independent experiments performed each in triplicate), *p<0.05 vs. untreated cells.

Supplemental Figure 2 Estradiol prevents murine T cells adhesion and migration across primary brain microvascular endothelial cells. A Adhesion of murine $CD3^+$ lymphocytes to primary brain microvascular endothelial cells following treatment with TNFα + IFNγ (both 10ng/ml) and/or estradiol (100nM). Data are mean ± SEM, n=3 (three independent

experiments, each performed in triplicate), *p<0.05 *vs.* unstimulated control, +p<0.05 *vs.* TNFα/IFNγ treatment alone. **B** Transmigration of murine $CD3^+$ lymphocytes across primary brain microvascular endothelial cells following treatment with TNFα + IFNγ (both 10ng/ml) and/or estradiol (100nM). Data are mean ± SEM, n=3 (three independent experiments, each performed in triplicate), *p<0.05 *vs.* unstimulated control, +p<0.05 *vs.* TNFα/IFNγ treatment alone.

Supplemental Figure 3 Validation of down regulation of ANXA1 expression in hCMEC/D3 cells following infection with shRNA. Representative western blot for selected clones (A-C) showing down-regulation of ANXA1 expression compared with mock infected cells (U) following stable infection with shRNA sequences targeting ANXA1.

FIGURE 1

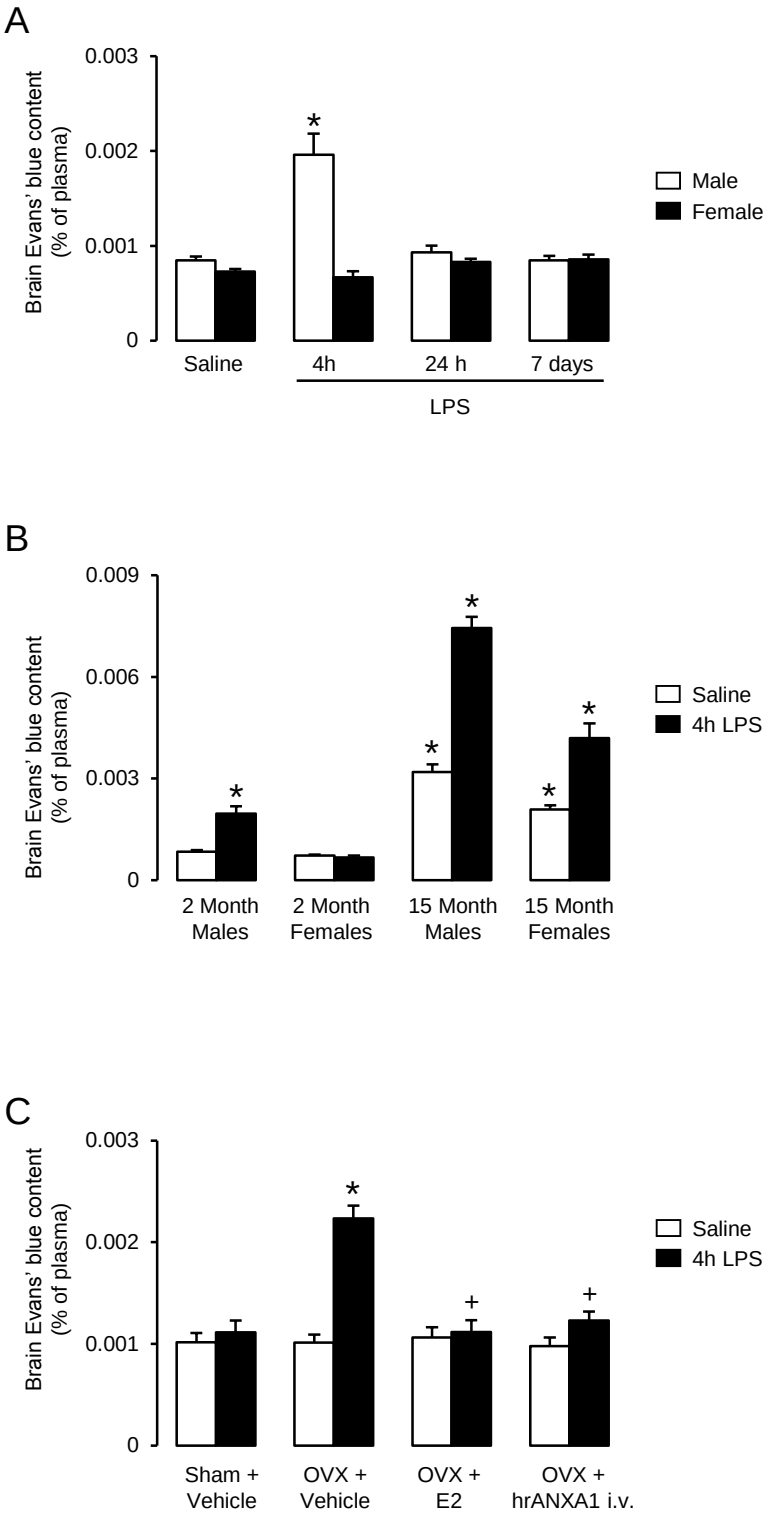
A
Brain Evans' blue content (% of plasma)
0.003
0.002
0.001
0
*
Male
Female
Saline
4h
24 h
7 days
LPS
B
Brain Evans' blue content (% of plasma)
0.009
0.006
0.003
0
*
Saline
4h LPS
2 Month Males
2 Month Females
15 Month Males
15 Month Females
C
Brain Evans' blue content (% of plasma)
0.003
0.002
0.001
0
*
+
Saline
4h LPS
Sham + Vehicle
OVX + Vehicle
OVX + E2
OVX + hrANXA1 i.v.

FIGURE 2-Amended

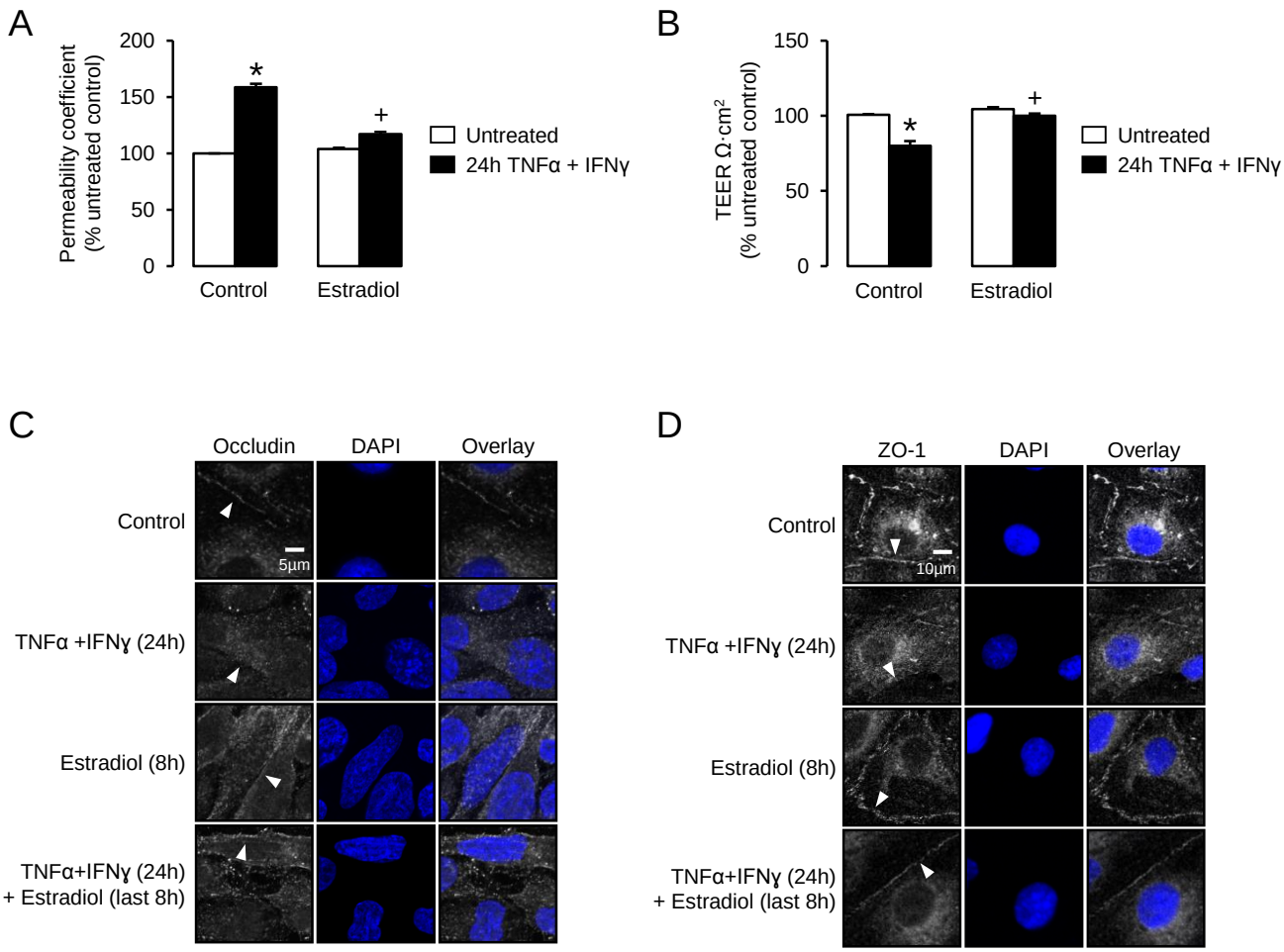

FIGURE 3

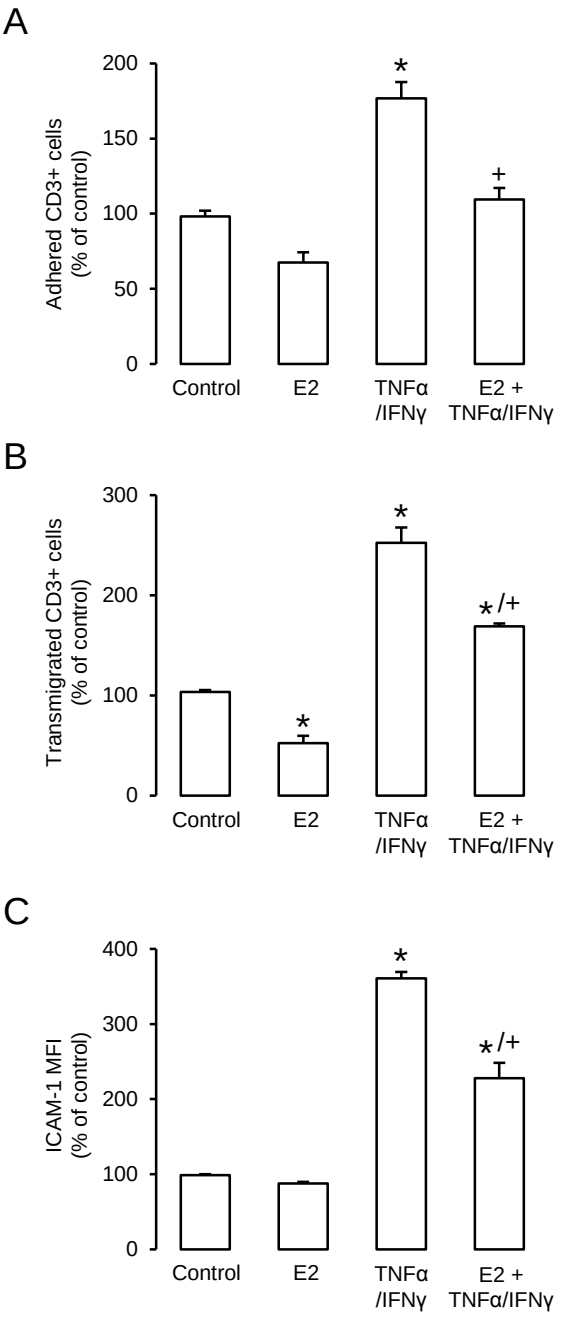
A
Adhered CD3+ cells
(% of control)
200
150
100
50
0
*
+
Control
E2
TNFα
/IFNγ
E2 +
TNFα/IFNγ
B
Transmigrated CD3+ cells
(% of control)
300
200
100
0
*
*
*/+
Control
E2
TNFα
/IFNγ
E2 +
TNFα/IFNγ
C
ICAM-1 MFI
(% of control)
400
300
200
100
0
*
*/+
Control
E2
TNFα
/IFNγ
E2 +
TNFα/IFNγ

FIGURE 4 Amended

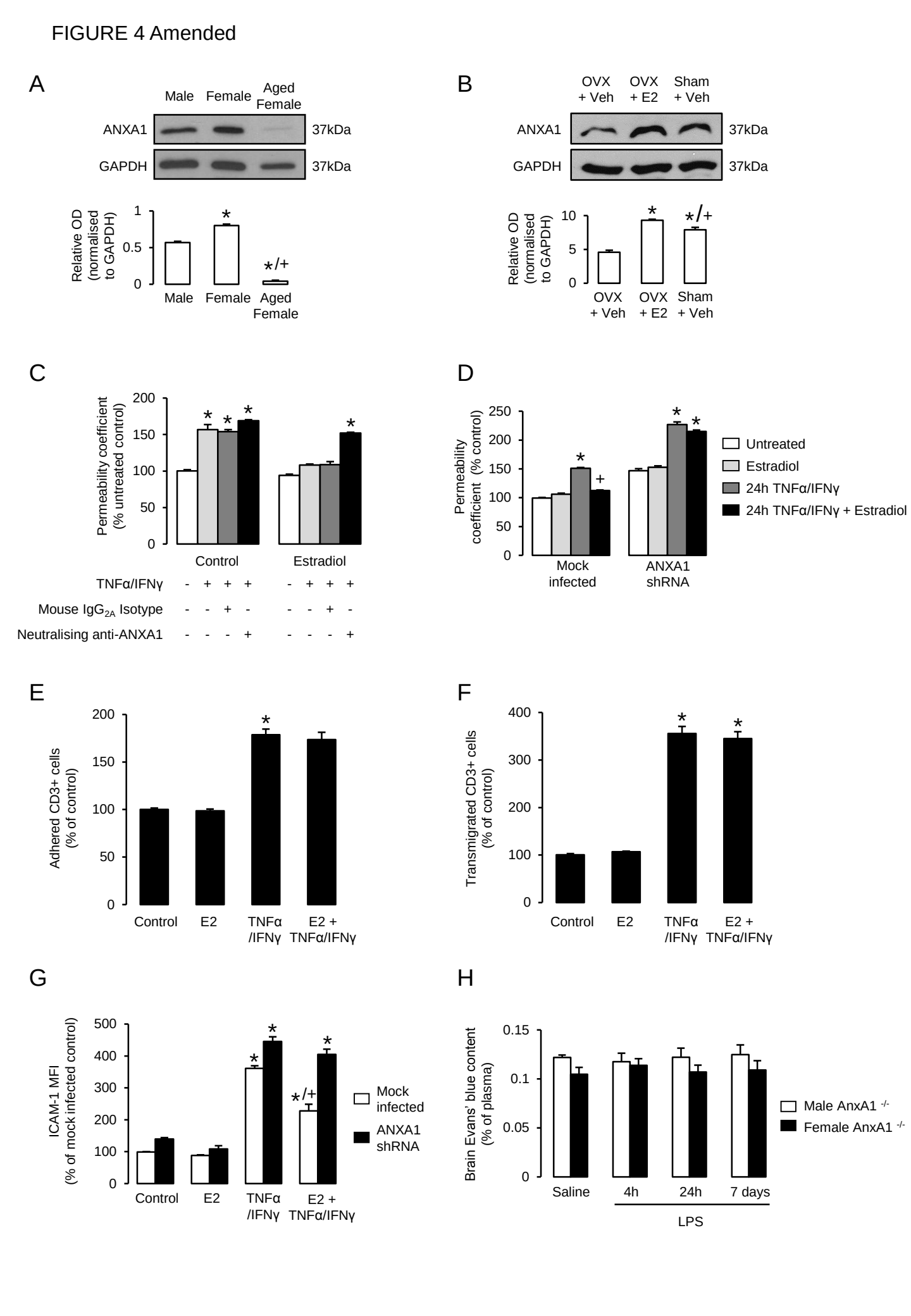

FIGURE 5

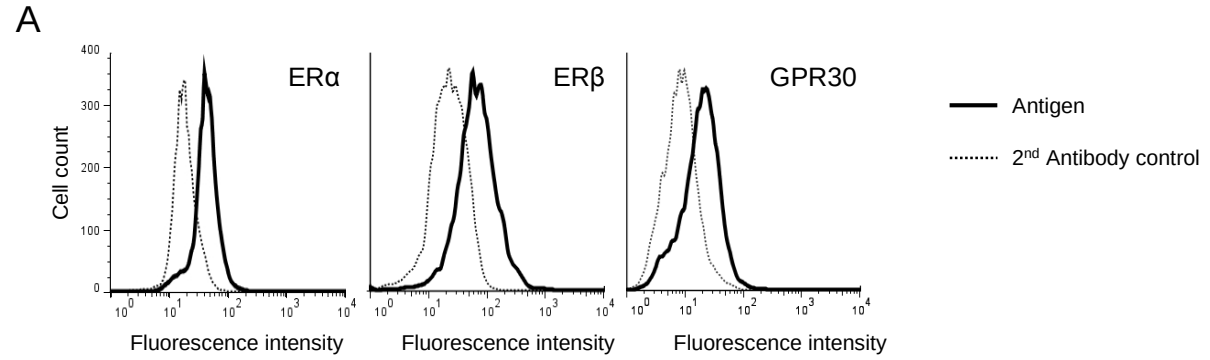
A
ERα
ERβ
GPR30
Cell count
Fluorescence intensity
Fluorescence intensity
Fluorescence intensity
Antigen
2nd Antibody control

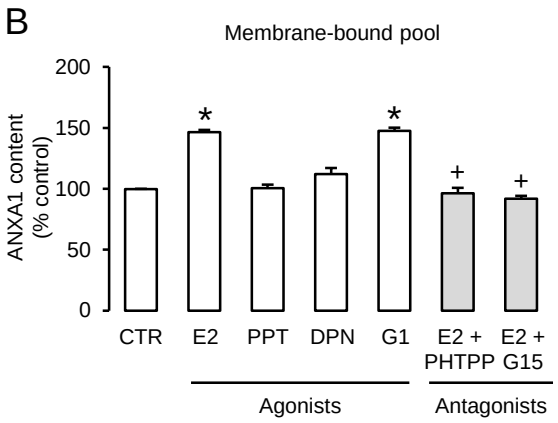
B
Membrane-bound pool
ANXA1 content (% control)
CTR
E2
PPT
DPN
G1
E2 + PHTPP
E2 + G15
Agonists
Antagonists

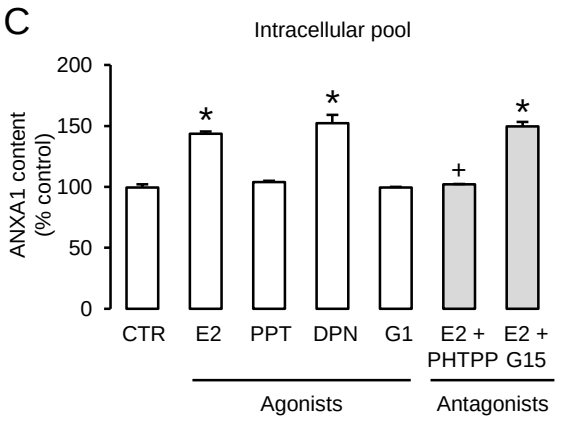
C
Intracellular pool
ANXA1 content (% control)
CTR
E2
PPT
DPN
G1
E2 + PHTPP
E2 + G15
Agonists
Antagonists

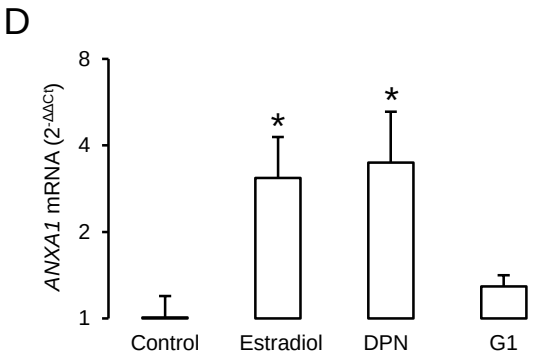
D
ANXA1 mRNA (2-ΔΔCt)
Control
Estradiol
DPN
G1

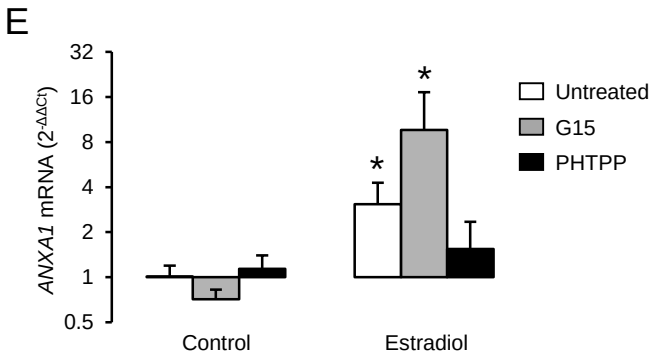
E
ANXA1 mRNA (2-ΔΔCt)
Control
Estradiol
Untreated
G15
PHTPP

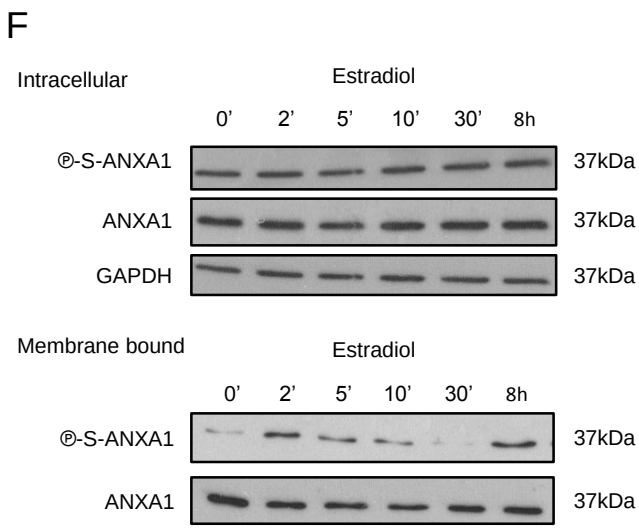
F
Intracellular
Estradiol
0'
2'
5'
10'
30'
8h
Ⓟ-S-ANXA1
ANXA1
GAPDH
37kDa
37kDa
37kDa
Membrane bound
Estradiol
0'
2'
5'
10'
30'
8h
Ⓟ-S-ANXA1
ANXA1
37kDa
37kDa

FIGURE 6

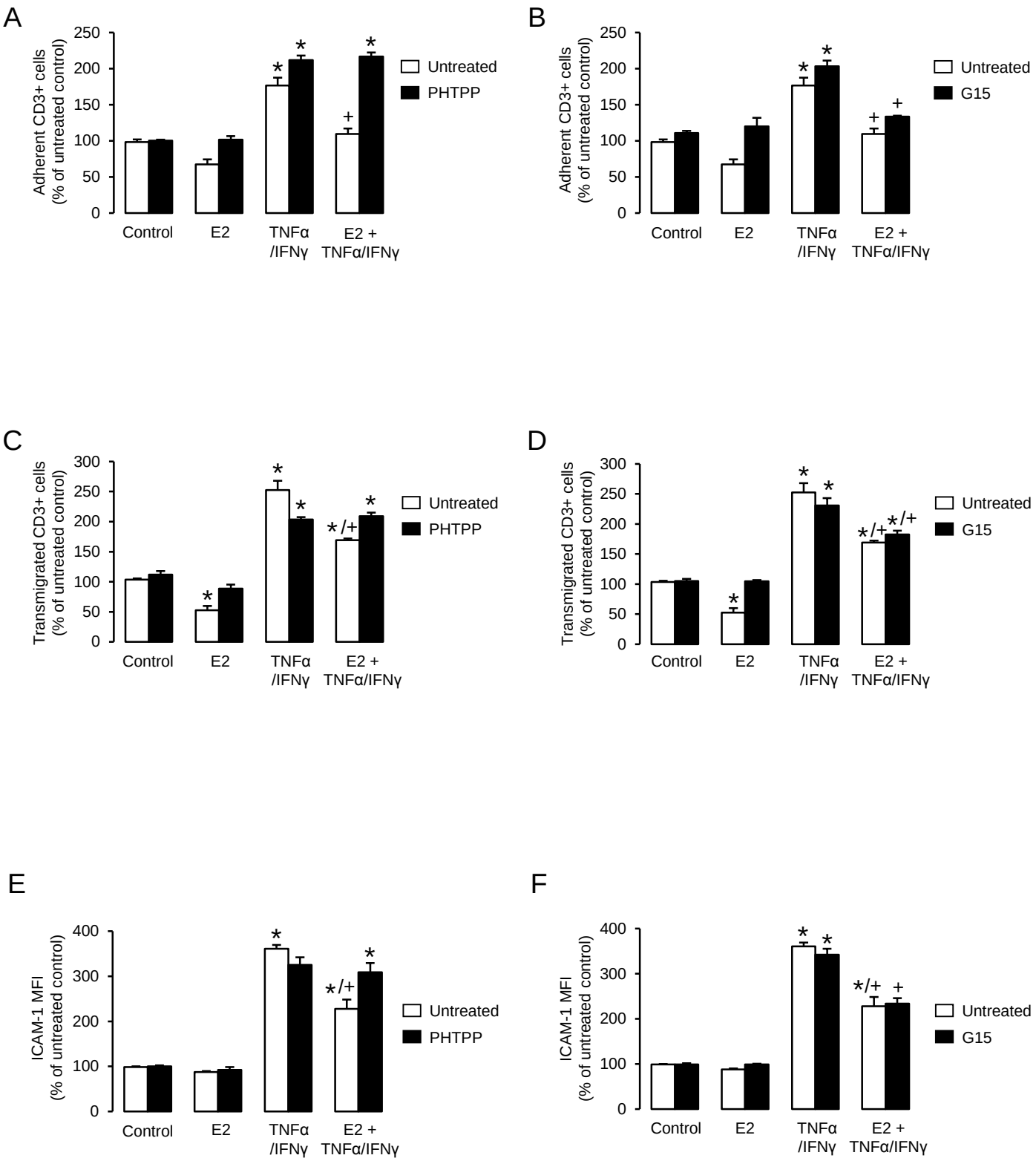
A
Adherent CD3+ cells
(% of untreated control)
250
200
150
100
50
0
Control
E2
TNFα
/IFNγ
E2 +
TNFα/IFNγ
Untreated
PHTPP
B
Adherent CD3+ cells
(% of untreated control)
Untreated
G15
C
Transmigrated CD3+ cells
(% of untreated control)
300
250
200
150
100
50
0
Untreated
PHTPP
D
Transmigrated CD3+ cells
(% of untreated control)
Untreated
G15
E
ICAM-1 MFI
(% of untreated control)
400
300
200
100
0
Untreated
PHTPP
F
ICAM-1 MFI
(% of untreated control)
Untreated
G15

FIGURE 7

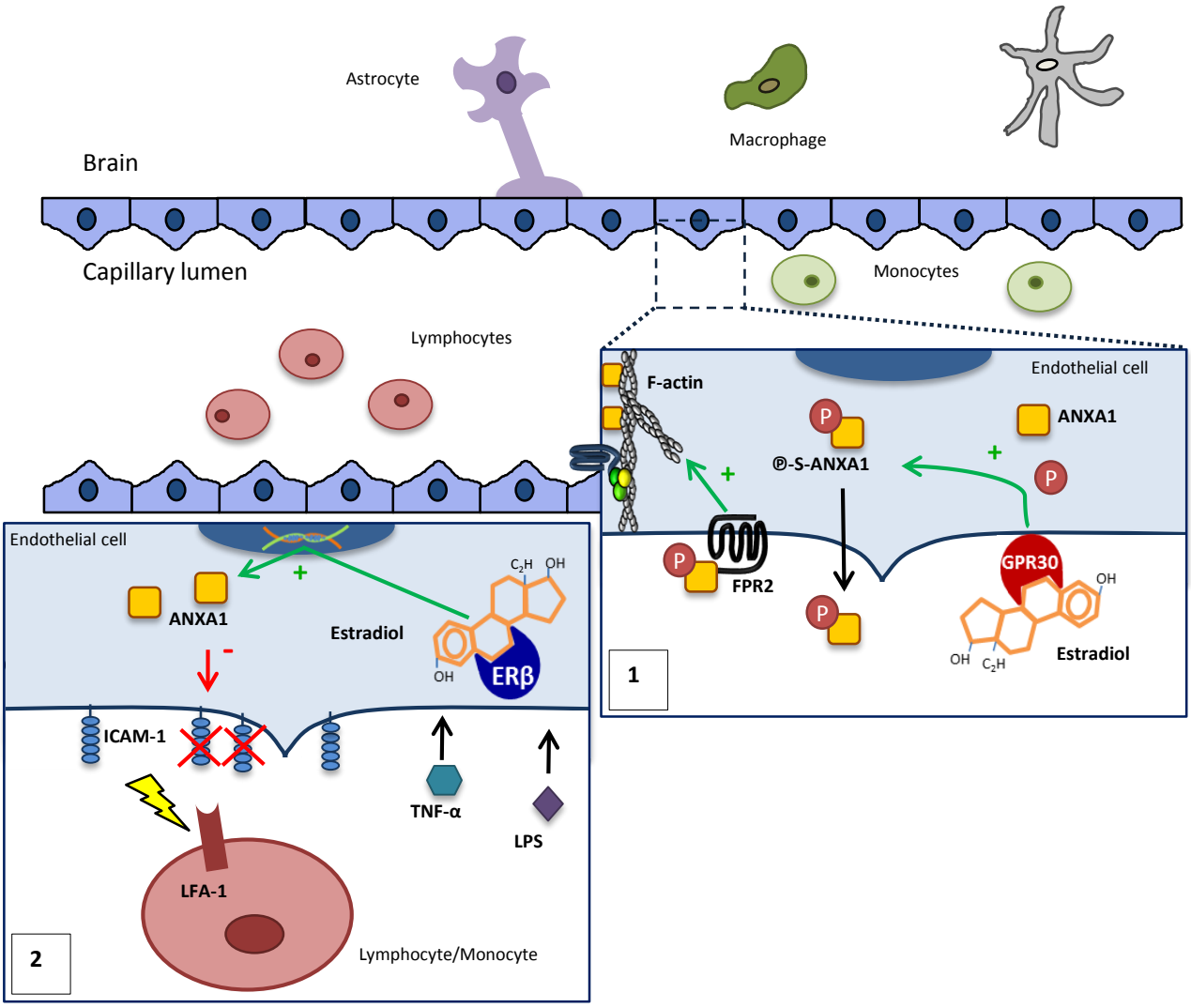
Astrocyte
Macrophage
Brain
Capillary lumen
Monocytes
Lymphocytes
Endothelial cell
F-actin
ANXA1
Ⓟ-S-ANXA1
FPR2
GPR30
Estradiol
1
Endothelial cell
ANXA1
Estradiol
ERβ
ICAM-1
TNF-α
LPS
LFA-1
Lymphocyte/Monocyte
2

Suppl. FIGURE 1

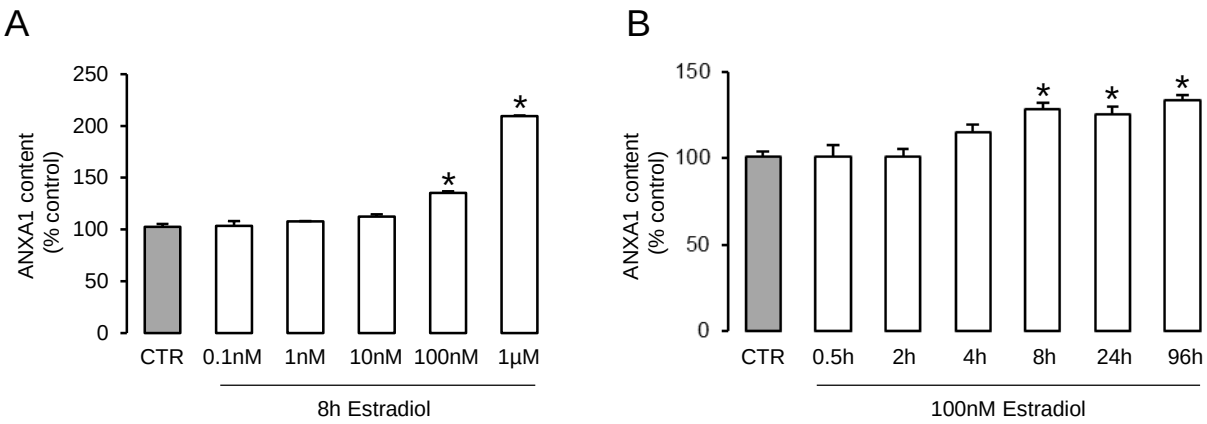

Suppl. FIGURE 2

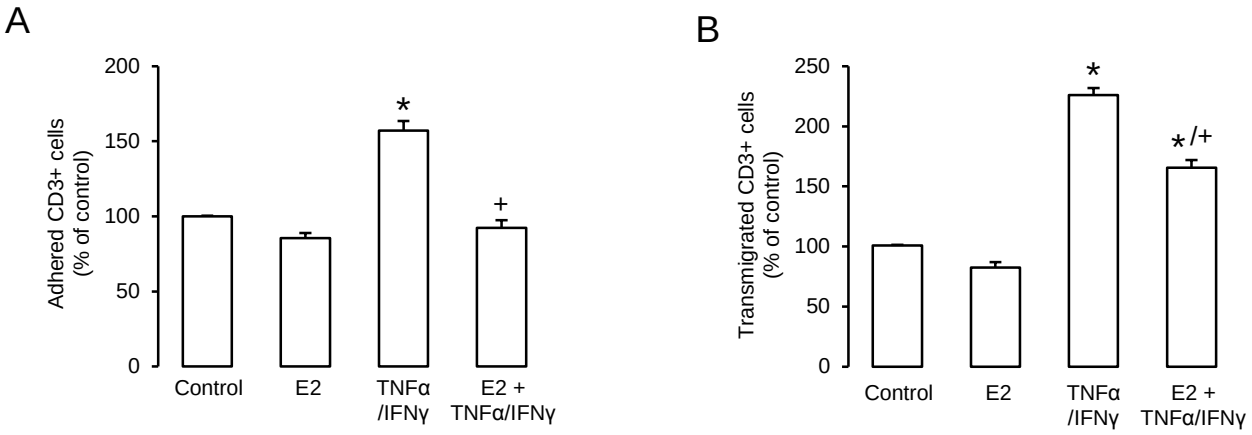

Suppl. FIGURE 3